PHYSICAL REVIEW B VOLUME 2, NUMBER 9 1 NOVEMBER 1970

Functional-Integral Approach to the Anderson Model for Dilute Magnetic Alloys from the Viewpoint of Diagrammatic Perturbation Technique*

Hellmut Keiter†
Department of Physics, University of Pennsylvania, Philadelphia, Pennsylvania 19104
(Received 22 May 1970)

The grand partition function for the Anderson model can be expressed as a Gaussian average over the partition function of a one-particle system in a fluctuating external potential. Though the zero-frequency approximation for this potential leads to the correct well-known two limits of the Anderson model, it turns out to be insufficient even for the first corrections to these limits. Combining diagrammatic techniques and the functional-integral approach, we use a new kind of perturbation theory in order to find approximations which fulfill the requirement of giving the first few corrections to *both* limits. They correspond to approximations in the functional integral, which take into account an infinite number of non-Gaussian fluctuations around the static frequency of the external field, and which thus are inaccessible by the usual treatment. In particular, the Kondo effect is shown to result from singularities in the particle-hole propagation. The analysis of the paper suggests that the use of one random field in the functional-integral approach leads to greater technical difficulties than encountered in other comparable many-body methods.

I. INTRODUCTION

Recently functional-integral methods have been applied to the Anderson model for a magnetic impurity.[1–5] They represent a many-body technique, originally invented by Stratonovich,[6] and completed by Hubbard[7] and by Mühlschlegel,[8] which essentially transforms the grand partition function of a physical system with a time-independent Hamiltonian containing two-particle interactions into a one-particle problem in time-dependent external fields, the amplitudes of which have to be averaged over with a Gaussian weight. One then has three major possibilities to treat the transformed problem. (i) One approximates the amplitudes of the external fields as Gaussian fluctuations.[9] (ii) One develops a feeling for the physical behavior of the time-dependent one-particle problem and guesses its Green's function.[10] (iii) One searches for certain frequencies of the external fields, which play a dominant role. The latter approach proved to be particularly useful in the treatment of the superconducting electron gas.[11] Here the BCS solution for the free energy follows from taking into account the zero frequency of the external field only.

This so-called "static approximation" can also be successfully applied to the functional-integral formulation of the Anderson model, as was first shown by Mühlschlegel.[4] In the static approximation, one obtains exactly the limits $U=0$ (corresponding to the case where the electrons are allowed to hop, without restrictions, beyond those imposed by the Pauli principle, on and off the impurity atom) and $V_{\vec{k}d}=0$ (corresponding to the case where one has band electrons and an impurity atom without interaction). This holds true for the "two-variable" version of the functional integral used by Mühlschlegel[4] and by Hamann[5] as well as for the "one-variable scheme" used by Evenson, Schrieffer, and Wang[1,2] and Schrieffer.[3] In the one-variable scheme, the static approximation of the grand partition function can be expressed as an integral over the amplitude of a static magnetic field, the integrand being a Gaussian weight factor and the grand partition function of a one-body system, representing impurity electrons in a Hartree-type magnetic field with a self-energy which accounts for the damping caused by interaction with the conduction electrons. The free energy, corresponding to the integrand, allows for an important physical interpretation of how one passes from the Pauli susceptibility regime over to a localized magnetic moment.[1,3] It is therefore tempting to consider the static approximation as a zeroth-order solution and improve it by adding Gaussian fluctuations of the nonzero-frequency field amplitudes. Since this approach proved to contain mathematical difficulties,[1-3] and was unsuccessful in obtaining exactly the first $|V_{\vec{k}d}|^2$-power corrections to the $V_{\vec{k}d}=0$ limit, we undertook the present study of comparing the functional-integral method with formally exact diagrammatic perturbation techniques.

The one-variable functional integral is related to perturbation theory with $-\frac{1}{2}U(n_{d\uparrow}-n_{d\downarrow})^2$ as a perturbation, while ordinarily[12,13] one starts from $Un_{d\uparrow}n_{d\downarrow}$. We therefore show briefly in Sec. III how the two expansions are related. Section IV contains a review of the one-variable functional-integral method applied to the Anderson model, while in Sec. V the relations between the functional integral and diagrams are established. We find that the static-approximation sums the contribution of any diagram

which results from zero energy transfer by the interactions. (There is a close connection between our result and the corresponding one for the two-variable scheme, obtained earlier by Dworin).[14] We then redefine the diagrams in such a way that we have only nonzero energy transfer by the interaction lines, but an additional self-energy contribution from the zero-frequency field amplitude in each propagator. We show that the Gaussian fluctuation approximation in the functional integral corresponds to summing the ring diagrams in the new series; however, these diagrams are unimportant in the large-U case. The most important class in that case is seen to be unobtainable from a finite-order approximation in the nonzero-frequency fluctuations in the functional integral.

In Sec. VI we exploit the fact that for finite $\beta U \gg \beta^2 |V_{\vec{k}d}|^2_{\rm av} \gg 1$, $(\beta = 1/kT)$, not only one single frequency (as in the static approximation) but all frequencies up to the order of $\beta|V|^2$ are important. We start from a renormalized static approximation and show how one can sum classes of diagrams in such a way that one obtains agreement with known low-order perturbation expansions in powers of $\beta|V|^2/U$ and $U/\beta|V|^2$. This is a new kind of perturbation technique which allows one to treat *both* limits of the Anderson model with one approximation. The Kondo effect (Sec. VII) is seen to result from a singularity in the particle-hole ladder series for opposite spin of the particle and the hole.

From our analysis it follows that in the Kondo regime the above-mentioned possibilities (i) and (iii) for treating the functional integral are insufficient. Moreover, the technical difficulties seem to be greater than in other many-body techniques.

II. BASIC FORMULAS

The Anderson Hamiltonian is particularly convenient for studying the behavior of magnetic impurities in metals. It is given by

$$H = H_0 + H_V + H' . \tag{1}$$

Here H_0 describes the host metal in a single-band approximation and a localized orbital on the impurity atom

$$H_0 = \sum_{\vec{k}\sigma} \epsilon_{\vec{k}\sigma} c^\dagger_{\vec{k}\sigma} c_{\vec{k}\sigma} + \sum_\sigma \epsilon_{d\sigma} c^\dagger_{d\sigma} c_{d\sigma}, \tag{2}$$

where

$$\epsilon_{\vec{k}\sigma} = \epsilon_{\vec{k}} - \sigma g \mu B, \quad \epsilon_{d\sigma} = \epsilon_d - \sigma g' \mu B, \tag{3}$$

are k- and d-electron energies, respectively, measured relative to the chemical potential. The magnetic field B appearing in the Zeeman terms in (3) has to be weak in the sense that $\vec{k}$ is still a good quantum number.

An electron, originally located at the d orbital, tends to hop on and off the conduction band. This effect is accounted for by

$$H_V = \sum_{\vec{k}\sigma} (V_{\vec{k}d} c^\dagger_{\vec{k}\sigma} c_{d\sigma} + V^\dagger_{\vec{k}d} c^\dagger_{d\sigma} c_{\vec{k}\sigma}). \tag{4}$$

If there are two electrons in the localized orbital, the intra-atomic Coulomb interaction drives them apart; so we include this effect in

$$H' = U n_{d\uparrow} n_{d\downarrow} = U c^\dagger_{d\uparrow} c_{d\uparrow} c^\dagger_{d\downarrow} c_{d\downarrow}. \tag{5}$$

There is an alternative way to write the Hamiltonian (1) which will be used in Sec. IV:

$$H = \bar{H}_0 + H_V + \bar{H}', \tag{6}$$

where

$$\bar{H}_0 = \sum_{\vec{k}\sigma} \epsilon_{\vec{k}\sigma} c^\dagger_{\vec{k}\sigma} c_{\vec{k}\sigma} + \sum_\sigma \bar{\epsilon}_{d\sigma} c^\dagger_{d\sigma} c_{d\sigma}, \tag{7}$$

$$\bar{H}' = -\tfrac{1}{2} U (n_{d\uparrow} - n_{d\downarrow})^2. \tag{8}$$

In deriving (6), we have shifted the d-electron energy by $\frac{1}{2}U$:

$$\bar{\epsilon}_{d\sigma} = \epsilon_{d\sigma} + \tfrac{1}{2} U, \tag{9}$$

and have used $(n_{d\sigma})^2 = n_{d\sigma}$.

For later purposes we introduce Green's functions[15]:

$$G_{AB}(\tau) = -\langle \mathcal{T} A(\tau) B(0) \rangle, \tag{10}$$

where

$$A(\tau) = e^{H\tau} A\, e^{-H\tau} \tag{11}$$

represents a Heisenberg operator and τ is an imaginary time. Fourier transforming (10), we have

$$\begin{aligned} G_{AB}(\tau) &= (1/\beta) \textstyle\sum_n e^{-i\omega_n \tau} G_{AB}(\omega_n) \\ &\equiv (1/\beta) \textstyle\sum_n e^{-i\omega_n \tau} \langle\langle A | B \rangle\rangle. \end{aligned} \tag{12}$$

Here ω_n is given by

$$\begin{aligned} \omega_n &= (2n+1)(\pi/\beta), \quad \text{for fermions,} \\ &= 2n\,(\pi/\beta), \quad \text{for bosons,} \end{aligned} \tag{13}$$

where $n = 0, \pm 1, \pm 2, \cdots$; and the fermion case applies if A and B obey a fermion-type commutation relation.

The most important Green's function for the following is given by

$$G^\sigma_{dd}(\tau) = -\langle \mathcal{T} c_{d\sigma}(\tau) c^\dagger_{d\sigma}(0) \rangle. \tag{14}$$

Its Fourier transform obeys the *exact* equation of motion

$$\begin{aligned} &[i\omega_n - \epsilon_{d\sigma} - \textstyle\sum_{\vec{k}} V^*_{\vec{k}d} V_{\vec{k}d} / (i\omega_n - \epsilon_{\vec{k}\sigma})] \langle\langle c_{d\sigma} | c^\dagger_{d\sigma} \rangle\rangle \\ &\quad = 1 + U \langle\langle c_{d\sigma} c^\dagger_{d\bar{\sigma}} c_{d\bar{\sigma}} | c^\dagger_{d\sigma} \rangle\rangle , \end{aligned} \tag{15}$$

where $\bar{\sigma} = -\sigma$.

It is convenient to introduce the abbreviation

$$S^\sigma(\omega_n) = \textstyle\sum_{\vec{k}} V^*_{\vec{k}d} V_{\vec{k}d} / (i\omega_n - \epsilon_{\vec{k}\sigma}) \equiv S^\sigma_n . \tag{16}$$

For a broad band and a slowly varying $V_{\vec{k}d}$, we shall

repeatedly use the approximation

$$S^{\sigma}(\omega_n) \approx -i\pi N(0)\overline{|V_{\vec{k}d}|^2}\,\mathrm{sign}\omega_n \equiv -i\Gamma\,\mathrm{sign}\omega_n \quad , \quad (17)$$

where $N(0)$ denotes the density of states near the Fermi surface.

The thermodynamic properties of the Anderson model are well known in two limits. Setting $H_V \equiv 0$ in (1), the remaining Hamiltonian can be immediately diagonalized. We then obtain for the grand partition function

$$Z[H_0+H'] = \mathrm{Tr}\, e^{-\beta(H_0+H')}$$

$$= Z_{\mathrm{Band}}\left(1+e^{-\beta\epsilon_{d\uparrow}}+e^{-\beta\epsilon_{d\downarrow}}+e^{-\beta(\epsilon_{d\uparrow}+\epsilon_{d\downarrow}+U)}\right) \quad . \quad (18)$$

Here we have indicated by the square bracket that Z is a functional of H_0+H'. From (18) the static magnetic susceptibility can be calculated via

$$\chi = \frac{1}{\beta}\frac{\partial^2 \ln Z}{\partial B^2} \quad (19)$$

This gives a Curie-type contribution from the impurity in addition to the Pauli susceptibility for the band electrons. On the other hand, a pure Pauli susceptibility is obtained if one sets $H' \equiv 0$ in (1). The corresponding grand partition function is given by

$$Z[H_0+H_V] = \mathrm{Tr}\, e^{-\beta(H_0+H_V)}$$

$$= Z_{\mathrm{Band}} \exp\Big[\sum_{\sigma\omega_n} e^{i\omega_n\delta} \ln(i\omega_n - \epsilon_{d\sigma} - S_n^{\sigma})\Big] \quad , \quad (20)$$

where δ is an infinitesimal positive quantity throughout this paper.

III. DIRECT PERTURBATION EXPANSIONS

Knowing the grand partition function in the above two limits, one can carry out perturbation expansions either in H_V[16] or in H'.[12,13] The former type of expansion leads to the Kondo effect in finite-order perturbation theory, the latter only after infinite summations have been carried out. The latter, however, has the advantage that the usual many-body formalism (Wick's theorem and linked-diagram expansions) can be immediately applied, and the expansion can be surveyed easily. That is why diagrammatic perturbation technique (in $\bar{H}'$ instead of H') will provide us with a tool to judge certain approximations in the functional-integral approach (Sec. IV). So we first have to establish the relation between the perturbation series in H' and $\bar{H}'$.

It is straightforward to write the grand partition function as

$$Z[H] = Z[H_0+H_V]\exp C \quad , \quad (21)$$

or

$$Z[H] = Z[\bar{H}_0+H_V]\exp\bar{C} \quad . \quad (22)$$

Here $Z[H_0+H_V]$ is given by (20), while

$$Z[\bar{H}_0+H_V] = Z_{\mathrm{Band}} \exp\Big[\sum_{\omega_n,\sigma} e^{i\omega_n\delta} \ln(i\omega_n - \bar{\epsilon}_{d\sigma} - S_n^{\sigma})\Big] \quad . \quad (23)$$

C and $\bar{C}$ stand for an infinite sum of topological distinct closed connected diagrams, which can be constructed according to the following rules.

Rules for C

In order to obtain the pth-order diagrams for C:

(a) Write down vertically p dashed interaction lines, each of them between two vertices. Then connect the vertices in all possible ways by full directed lines, one entering and one leaving each vertex. The full lines may form between 2 and $p+1$ closed loops, subject to the restriction that an interaction line must connect different loops with opposite spins (see below).

(b) The full lines carry a frequency ω_n and a spin σ, which is the same for all full lines forming a closed loop. A full line stands for

$$G^{\sigma}_{0\,dd}(\omega_n)e^{i\omega_n\delta} = [i\omega_n - \epsilon_{d\sigma} - S^{\sigma}(\omega_n)]^{-1}e^{i\omega_n\delta} \quad , \quad (24)$$

where δ is positive infinitesimal.

(c) An interaction line connects two vertices belonging to two loops with opposite spin. It stands for $\frac{1}{2}U\sigma\bar{\sigma}$.

(d) The single diagram carries an over-all factor $(-1)^F\beta/S$, where F denotes the number of closed loops, and S is the symmetry factor of the diagram (for S see the rules for the diagrams for $\bar{C}$).

(e) There is frequency conservation at each vertex. Sum over all independent frequencies (each sum with a factor $1/\beta$) and over the two spin directions.

Rules for $\bar{C}$

In order to obtain the pth-order diagram for $\bar{C}$:

($\bar{\mathrm{a}}$) Act according to rule (a); however, disregard the restrictions mentioned there.

($\bar{\mathrm{b}}$) A full line carries a frequency ω_n and a spin σ, which is the same for all full lines forming a closed loop. A full line stands for

$$\bar{G}^{\sigma}_{0\,dd} = [i\omega_n - \bar{\epsilon}_{d\sigma} - S^{\sigma}(\omega_n)]^{-1} \quad . \quad (25)$$

($\bar{\mathrm{c}}$) An interaction line may connect any two vertices. It stands for $\frac{1}{2}U\sigma\sigma'$.

($\bar{\mathrm{d}}$) The over-all factor is the same as in (d). The symmetry factor S of a diagram is obviously the same as for the diagram in the perturbation expansions for a gas of electrons interacting via two-body Coulomb forces, and can be found in the standard textbooks.

($\bar{\mathrm{e}}$) There is frequency conservation at each vertex. Sum over all independent frequencies (each sum with a factor $1/\beta$) and over all spins. Some of the diagrams are shown in Fig. 1.

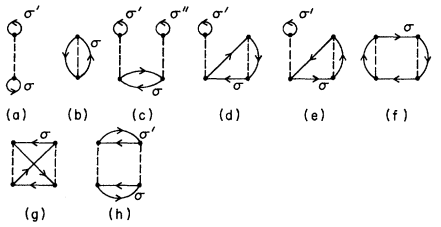

FIG. 1. All first-order and some characteristic second-order diagrams in the $\bar{H}'$ expansion.

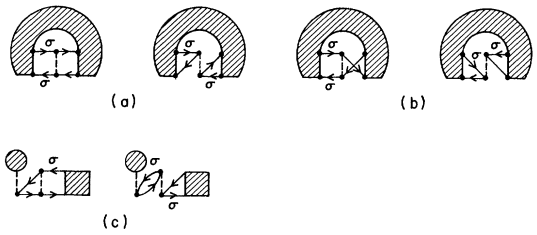

FIG. 3. Three pairs of canceling diagrams.

($\bar{f}$) Compared with the well-known rules for the interacting electron gas, there are some minor modifications. Using (25), the diagrammatic part drawn in Fig. 1(b), for example, contains a frequency sum, which does not converge. However, specifying the basic interaction as indicated in Fig. 2, we see that the ascending line of diagram 1(b) represents $\bar{G}^{\sigma}_{0\,dd}(\omega_n)e^{-i\omega_n\delta}$, while the descending line of diagram 1(b) as well as the balloon-diagram line in 1(a) and 1(c) represent $\bar{G}^{\sigma}_{0\,dd}(\omega_n)e^{i\omega_n\delta}$, where δ is positive infinitesimal.

After having established the rules for the two different diagrammatic expansions we turn to comparing them. We first observe that $\bar{C}$ contains many more topological structures than C, as a result of having artificially written in $\bar{H}'$ a part of the one-body interaction in terms of a two-body interaction between electrons of equal spin. Consequently, the pure many-body part of this interaction between equal spin electrons, i. e., the part exceeding the Hartree-Fock interaction, has to drop out in the diagrams for $\bar{C}$. Consider, e. g., the diagrams of Fig. 3. The second diagram in Fig. 3(a) or Fig. 3(b), respectively, contains one closed loop more or one less than the first diagram. Otherwise their contribution is the same, so they cancel each other; similarly, diagram 1(g) and that part of 1(h) where $\sigma=\sigma'$ cancel each other. So we are left with all diagrams or parts of diagrams, which contain only

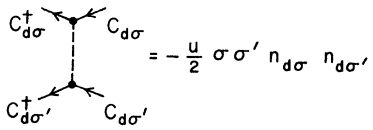

FIG. 2. Basic interaction in the $\bar{H}'$ expansion. Special form of the interaction requires specification of the relative position of the two operators $n_{d\sigma}$ and $n_{d\sigma'}$ in the diagrams. The convention we use is to place the first operator $n_{d\sigma}$ of the interaction always above the second operator $n_{d\sigma'}$ in the vertically drawn interaction line. The same effect could be produced by assigning an arrow to the interaction line.

Hartree-Fock interactions between equal spins (in addition to the interaction between opposite spins). The one-body character of this interaction can be seen more clearly, if we add the four diagrams (a)-(d), shown in Fig. 4, obtaining (e). Here the dot stands for

$$(U/2\beta)\sum_{\omega_n}\bar{G}^{\sigma}_{0\,dd}(\omega_n)(e^{-i\omega_n\delta}+e^{i\omega_n\delta}-2e^{i\omega_n\delta})=-\tfrac{1}{2}U\ . \tag{26}$$

Viewed as a self-energy, the dot renormalizes $\bar{G}^{\sigma}_{0\,dd}(\omega_n)$:

$$\bar{G}^{\sigma}_{0\,dd}(\omega_n)[1+\tfrac{1}{2}U\bar{G}^{\sigma}_{0\,dd}(\omega_n)]^{-1}=(i\omega_n-\bar{\epsilon}_{d\sigma}+\tfrac{1}{2}U-S^{\sigma}_n)^{-1}$$
$$=G^{\sigma}_{0\,dd}(\omega_n)\ . \tag{27}$$

Such a renormalization can be carried out only in those diagrams, which contain a genuine many-body interaction (i. e., at least one interaction line between opposite spins), for only there the diagram without Hartree-Fock inclusions for equal spin (i.e., the diagram with $\bar{G}^{\sigma}_{0\,dd}$ lines) and the same diagram with $\bar{G}^{\sigma}_{0\,dd}$ replaced by $G^{\sigma}_{0\,dd}$ contain the same symmetry factor S. Obviously the sum of all genuine renormalized many-body diagrams is given by C.

So we are left with all diagrams which contain nothing but Hartree-Fock interactions between equal spins. Adding the corresponding contributions from Figs. 1 (a) and 1 (b) for the first-order terms in U, as well as the higher-order terms, which can be obtained by applying the reduction scheme outlined in Fig. 4, we get

$$\tfrac{1}{2}U\sum_{\omega_n,\sigma}e^{i\omega_n\delta}\bar{G}^{\sigma}_{0\,dd}(\omega_n)-\tfrac{1}{2}(\tfrac{1}{2}U)^2\sum_{\omega_n,\sigma}[\bar{G}^{\sigma}_{0\,dd}(\omega_n)]^2$$
$$+\tfrac{1}{3}(\tfrac{1}{2}U)^3\sum_{\omega_n,\sigma}[\bar{G}^{\sigma}_{0\,dd}(\omega_n)]^3\pm\ldots$$

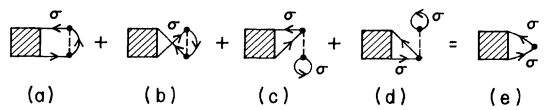

FIG. 4. Reduction of the Hartree-Fock interaction among equal spins to a one-body interaction.

$$= \sum_{\omega_n,\sigma} e^{i\omega_n\delta} \ln[1+\tfrac{1}{2}U\overline{G}^{\sigma}_{0\,dd}(\omega_n)] \ , \qquad (28)$$

whereupon

$$e^{\overline{C}} = e^{C} \exp\{\sum_{\omega_n,\sigma} e^{i\omega_n\delta} \ln[1+\tfrac{1}{2}U\overline{G}^{\sigma}_{0\,dd}(\omega_n)]\} \qquad (29)$$

follows. Inserting (29) into (22) and using (23), we obtain the desired expression (21).

Summarizing the above results, we have been able to map the diagrammatic expansion with $\overline{H}'$ as perturbation onto the diagrammatic expansion with H' as perturbation because of the following three facts, which hold for the $\overline{H}'$ expansion. (i) Diagrammatic parts with a genuine many-body interaction between equal spins cancel each other. (ii) The remaining Hartree-Fock–type interaction between equal spins can be used to renormalize the electron lines in all diagrams which contain interactions between opposite spins. (iii) The diagrams which contain only Hartree-Fock–type interaction between equal spins and no interactions between opposite spins can be summed to give a correction factor for the zero-order grand partition function.

We conclude Sec. III by sketching how one can obtain self-consistent approximations for the grand partition function from the diagrammatic point of view.[17] For that purpose we define a self-energy part for the exact Green's function (14) with the aid of the equation of motion (15):

$$U\langle\langle c_{d\sigma}c^{\dagger}_{d\bar{\sigma}}c_{d\bar{\sigma}}|c^{\dagger}_{d\sigma}\rangle\rangle \equiv \Sigma^{\sigma}_{dd}(\omega_n)\langle\langle c_{d\sigma}|c^{\dagger}_{d\sigma}\rangle\rangle \ . \qquad (30)$$

Expanding $G^{\sigma}_{dd}(\omega_n)$ in terms of diagrams using H' as a perturbation, $\Sigma^{\sigma}_{dd}(\omega_n)$ is given by a set of irreducible diagrams. From these diagrams we pick up all skeleton diagrams with k interaction lines and replace the electron lines, which stand for $G^{\sigma}_{0\,dd}(\omega_n)$, by $G^{\sigma}_{dd}(\omega_n)$. Denoting the sum of these renormalized skeleton diagrams by $\Sigma^{\sigma(k)}_{dd}(\omega_n)$, we have

$$\Sigma^{\sigma}_{dd}(\omega_n) = \sum_k \Sigma^{\sigma(k)}_{dd}(\omega_n) \ . \qquad (31)$$

Let Ω' be defined by

$$\Omega' = \sum_{\sigma}(1/\beta)\sum_{\omega_n} e^{i\omega_n\delta}\sum_k (1/2k)\,\Sigma^{\sigma(k)}_{dd}(\omega_n)\,G^{\sigma}_{dd}(\omega_n) \ . \qquad (32)$$

Then, applying Ambegaokar's[17] proof, it can be shown that the thermodynamic potential Ω can be expressed as

$$\Omega \equiv -(1/\beta)\ln Z[H]$$

$$= \Omega' - (1/\beta)\sum_{\sigma,\omega_n} e^{i\omega_n\delta}[\Sigma^{\sigma}_{dd}(\omega_n)G^{\sigma}_{dd}(\omega_n) - \ln G^{\sigma}_{dd}(\omega_n)]$$

$$-(1/\beta)\ln Z_{\text{Band}} \ . \qquad (33)$$

The obvious advantage of (33) is that an approximation for $\Sigma^{\sigma}_{dd}(\omega_n)$ defines uniquely an approximation for Ω, if the Dyson relation [following from (15) and (30)] between $G^{\sigma}_{dd}(\omega_n)$ and $\Sigma^{\sigma}_{dd}(\omega_n)$ is kept.[18] In principle, (33) can be used later as a guide for finding appropriate approximations in the present problem, using combined perturbation-technical and functional-integral methods.

IV. FUNCTIONAL-INTEGRAL METHOD

Whenever the two-body–interaction part of a Hamiltonian can be written as a square of one-body operators [as $\overline{H}'$ in Eq. (8)], the identity[6,7]

$$\exp(a^2) = \int_{-\infty}^{\infty} \exp(-x^2+2ax)\,dx/\sqrt{\pi} \qquad (34)$$

can be used to reduce the two-body interaction [a^2 in (34)] to a one-body interaction with a time-varying external field, which has to be averaged over with a Gaussian weight. For that purpose we use the Hamiltonian in the form (6) with (7) and (8), following closely the work in Refs. 1–3. It should be mentioned that this is not the only way to apply functional-integral methods to the present problem. There are other possibilities for writing the two-body interaction as a sum of squares of one-body operators.[4,2] One of them has been used by Hamann.[5]

We feel at present that starting from (6) is the simplest mathematical way, and the way which permits the easiest physical interpretation of the results. Furthermore, this way will show some drawbacks of the functional-integral method most clearly.

The identity (34) can be applied directly to the right-hand side of

$$\exp[-\beta(\overline{H}_0+H_V+\overline{H}')]$$

$$= \mathcal{T}\exp[-\beta\int_0^1(\overline{H}_{0\tau}+H_{V\tau}+\overline{H}'_{\tau})\,d\tau] \ , \qquad (35)$$

since, having introduced a Feynman time ordering, the operators can be treated as c numbers. We obtain[19]

$$Z[H] = \int \mathfrak{D}\,\xi(\tau)\exp[-\pi\int_0^1 d\tau\,\xi^2(\tau)]\,\mathrm{Tr}\,\mathcal{T}$$

$$\times\exp\{-\int_0^1 d\tau[\beta\overline{H}_{0\tau}+\beta H_{V\tau}-c\,\xi(\tau)\textstyle\sum_{\sigma}\sigma n_{d\sigma\tau}]\} \ . \qquad (36)$$

Here $\xi(\tau)$ is the "random" field, corresponding to x in (34), c is given by $c=(2\pi\beta U)^{1/2}$, and the average has to be taken over all possible random fields with a Gaussian weight.

As was shown in Refs. 1–3, the grand partition function (36) can be further transformed. Using the Fourier transformation

$$\xi(\tau) = \sum_{\nu=-\infty}^{\infty}\xi_{\nu}e^{-i\Omega_{\nu}\tau}, \quad \Omega_{\nu}=2\pi\nu \ , \quad \xi_{\nu}=\xi^{*}_{-\nu} \qquad (37)$$

where ν is an integer, and expressing $n_{d\sigma\tau}$ via nonequilibrium Green's-function techniques, one obtains

$$Z[H] = Z[\bar{H}_0 + H_V]\int_{-\infty}^{\infty} d\xi_0 \int \prod_{\nu>0} (2d^2\xi_\nu) \exp\left(-\pi \sum_{\nu'=-\infty}^{\infty} |\xi_{\nu'}|^2\right) \times \exp\left\{\sum_{\sigma,n} e^{i\omega_n\delta} \langle n | \ln[1 + (\sigma c/\beta)\xi \bar{G}^{\sigma}_{0\,dd}] | n\rangle\right\} . \quad (38)$$

Here $Z[\bar{H}_0 + H_\nu]$ is given by (23). The operator inside the brackets in (38) can be represented by its matrix elements in frequency space

$$(\sigma c/\beta)\langle m | \xi \bar{G}^{\sigma}_{0\,dd} | n\rangle = (\sigma c/\beta)\, \xi_{m-n}\, \bar{G}^{\sigma}_{0\,dd}(\omega_n) , \quad (39)$$

where $\bar{G}^{\sigma}_{0\,dd}(\omega_n)$ is given by (25) and ξ_{m-n} is the $(m-n)$th Fourier component of the random field (37). In (38) the zero frequency can be treated in a special way. Defining the "static grand partition function" via

$$Z_{\text{static}}(\xi_0) = \exp\left\{\sum_{n,\sigma} e^{i\omega_n\delta} \ln[1 + (\sigma c/\beta)\,\xi_0\, \bar{G}^{\sigma}_{0\,dd}(\omega_n)]\right\} , \quad (40)$$

one can rewrite $Z[H]$ as

$$Z[H] = Z[\bar{H}_0 + H_V]\int_{-\infty}^{\infty} d\xi_0\, e^{-\pi\xi_0^2} Z_{\text{static}}(\xi_0) \times \left\{\int \prod_{\nu>0} (2d^2\xi_\nu) \exp\left(-\pi \sum_{\nu'=-\infty;\,\nu'\neq 0}^{\infty} |\xi_{\nu'}|^2\right) \times \exp\left[\sum_{\sigma} \operatorname{Tr} \ln(1 - K^{\sigma})\right]\right\} . \quad (41)$$

The curly bracket in (41) represents the grand partition function of the fluctuations $\xi_\nu (\nu \neq 0)$ around a fixed Hartree magnetic field $c\xi_0$. The operator K^{σ} contains the fluctuations as a potential and $c\xi_0$ as a self-energy. It can be written as a matrix in frequency space:

$$K^{\sigma}_{mn} = -\sigma c \xi_{m-n}\, (1 - \delta_{m,n})\, (1/\beta)\, \tilde{G}^{\sigma}_n , \quad (42)$$

where

$$\tilde{G}^{\sigma}_n = [i\omega_n - \bar{\epsilon}_{d\sigma} + (\sigma c \xi_0/\beta) - S^{\sigma}(\omega_n)]^{-1} . \quad (43)$$

The advantage of representing $Z[H]$ by (41) was first recognized by Mühlschlegel,[4] who replaced the curly bracket by 1 and showed that this static approximation reproduces (18) in the limit $V_{kd} = 0$, and (20) in the limit $U = 0$.

In fact, for $U = 0$, we have $Z_{\text{static}}(\xi_0) = 1$, all ξ_ν integration give 1, and $Z[\bar{H}_0 + H_V]$ reduces to $Z[H_0 + H_V]$. The case $V_{kd} = 0$ is a bit more complicated. From (25) and (40) we have, quite generally,

$$Z[\bar{H}_0 + H_V]\, Z_{\text{static}}(\xi_0) = Z_{\text{Band}} \exp\left[\sum_{\sigma,\omega_n} e^{i\omega_n\delta} \ln(\tilde{G}^{\sigma}_n)^{-1}\right] . \quad (44)$$

The sum on the right-hand side of (44) can be evaluated by contour integral techniques.[20] For $V_{kd} = 0$, we have

$$\sum_{\omega_n\sigma} e^{i\omega_n\delta} \ln(i\omega_n - \bar{\epsilon}_{d\sigma} + \sigma c\xi_0/\beta) = \sum_{\sigma} \ln(1 + \exp\{-\beta[\bar{\epsilon}_{d\sigma} - (\sigma c/\beta)\xi_0]\}) . \quad (45)$$

Then, in the static approximation for $V_{kd} = 0$, the grand partition function

$$Z[H_0 + H'] \to \int_{-\infty}^{\infty} d\xi_0\, Z_{\text{Band}}\, e^{-\pi\xi_0^2} \times (1 + e^{-\beta\bar{\epsilon}_{d\uparrow} + c\xi_0})(1 + e^{-\beta\bar{\epsilon}_{d\downarrow} - c\xi_0}) = Z_{\text{Band}}(1 + e^{-\beta\epsilon_{d\uparrow}} + e^{-\beta\epsilon_{d\downarrow}} + e^{-\beta(\epsilon_{d\uparrow} + \epsilon_{d\downarrow} + U)}) \quad (46)$$

is in accord with (18).

The static grand partition function (40) can be calculated quite generally, if we approximate $S^{\sigma}(\omega_n)$ as in (17). The corresponding expression is given in the Appendix. For $\beta\Gamma \gg 1$ and in the symmetric case for zero magnetic field ($\bar{\epsilon}_{d\sigma} = 0$), we obtain

$$Z_{\text{static}}(\xi_0) \to \exp\left\{\frac{2c\xi_0}{\pi} \tan^{-1}\left(\frac{c\xi_0}{\pi\Gamma}\right) - \frac{\beta\Gamma}{\pi} \times \ln\left[1 + \left(\frac{c\xi_0}{\beta\Gamma}\right)^2\right]\right\} . \quad (47)$$

The corresponding free energy

$$\beta F(\xi_0) = -\ln Z_{\text{static}}(\xi_0) + \pi\xi_0^2 \quad (48)$$

shows a continuous change from a Pauli-susceptibility regime to a locally exchange-enhanced Pauli-susceptibility regime up to a strongly localized-moment regime, as has been discussed in detail in Refs. 1–3. (See, e.g., Fig. 1 of Ref. 1.) Unfortunately, however, the first corrections, in Γ/U or U/Γ, respectively, predicted by the static approximation, are not given correctly, as may be seen in Sec. V more easily than by direct calculation. Therefore the authors of Refs. 1–3 improved the static approximation by including Gaussian fluctuations around the Hartree field $c\xi_0$. For that purpose they expanded $\operatorname{Tr}\ln(1 - K^{\sigma})$ in (41) as

$$\textstyle\sum_{\sigma} \operatorname{Tr}\ln(1 - K^{\sigma}) \approx -\frac{1}{2}\sum_{\sigma} \operatorname{Tr}(K^{\sigma})^2 . \quad (49)$$

The linear term in K^{σ} vanishes because of (42). The approximation (49) resembles the well-known random phase approximation, and is called RPA′ in Refs. 1–3. Using the explicit expression (42) for K^{σ}, one has

$$-\tfrac{1}{2}\sum_{\sigma} \operatorname{Tr}(K^{\sigma})^2 = \tfrac{1}{2} \sum_{\sigma,\nu\neq 0} c^2 \varphi^{\sigma}_{\nu} |\xi_\nu|^2 , \quad (50)$$

with

$$\varphi^{\sigma}_{\nu} = -(1/\beta^2)\sum_{n} \tilde{G}^{\sigma}_{n} \tilde{G}^{\sigma}_{n+\nu} . \quad (51)$$

The sum (51) is calculated in the Appendix. For zero magnetic field, $\beta\Gamma \gg 1$ and in the symmetric case we obtain

$$\varphi_\nu = \tfrac{1}{2}\sum_{\sigma} \varphi^{\sigma}_{\nu} = \frac{\beta\Gamma}{\pi(|\Omega_\nu| + 2\beta\Gamma)|\Omega_\nu|} \times \ln\left(1 + \frac{|\Omega_\nu|(|\Omega_\nu| + 2\beta\Gamma)}{\beta^2\Gamma^2 + c^2\xi_0^2}\right) , \quad (52)$$

where $\Omega_\nu = 2\pi\nu$.

Obviously the approximation (49) can be viewed as an expansion in terms of ξ_ν, the amplitudes of the random field. However, whether we are allowed to chop the fluctuations at this Gaussian stage depends strongly on the randomness in time *and space* of the external field. If we had in addition to the random time dependence of the field a *spatial* randomness, as in the electron gas with Coulomb interactions between the electrons, the above expansion would correspond to a random-phase approximation for the *spatial* correlations, and the coefficients of terms like $|\xi_\nu|^2|\xi_\mu|^2$ with $\mu \neq \nu$ would be small compared to those of $|\xi_\nu|^2$. In the present problem, however, we deal with *spatially localized* interactions. Consequently, the approximation (47) need not be a good one, unless c is so small that the higher-order coefficients ($\sim c^4$, etc.) are negligible. So, from the foregoing interpretation, we may expect that the RPA′ [Eq. (49)] is a good approximation only for small c in the above sense. That this is indeed the case follows from the fact that the RPA′ gives the correct coefficient for the U/Γ expansion for the susceptibility. It does not give the Γ/U limit correctly. Moreover, it shows a mathematical breakdown: Calculating the curly bracket in (41), using (47), we obtain

$$Z[H] \to Z[\overline{H}_0 + H_V] \int_{-\infty}^{\infty} d\xi_0 Z_{\text{static}}(\xi_0) \times \prod_{\nu>0} [1 - (c^2/\pi)\varphi_\nu(\xi_0)]^{-1} . \quad (53)$$

If c^2 is of the order of $\beta\Gamma$, a pole occurs in (53), the position of which depends on ν and ξ_0.

In order to avoid this mathematical breakdown of the RPA′, one could think of including quartic fluctuations.[21] As we shall see from Sec. V, one cannot get the correct Γ/U limit in this case.

A further possibility is to calculate the coefficient in front of $|\xi_\nu|^2$ by means of variational methods, following the ideas of Mühlschlegel and Zittartz,[22] who applied the functional integral to the Ising model. An attempt in this direction undertaken by the present author showed that one can obtain the correct Γ/U limit, but it is likely that one obtains a mathematical breakdown analogous to the one in RPA′.

This completes our review of the application of pure functional-integral methods to the present problem and shows the need for an understanding of the above approximations by means of comparison with formally exact methods. So we turn to establish the relation between functional integrals and perturbation expansions.

V. RELATIONS BETWEEN FUNCTION-INTEGRAL AND DIAGRAMMATIC PERTURBATION EXPANSIONS

In (38), we expand the exponential function, which has to be averaged with a Gaussian weight, in a multiple power series in ξ_ν. Defining x_k by

$$x_k = -\sum_{\sigma,n} e^{i\omega_n\delta}(1/k)\langle n|[(\sigma c/\beta)\xi\overline{G}^\sigma_{dd}]^k|n\rangle , \quad (54)$$

and abbreviating the Gaussian average by brackets, we have

$$\frac{Z[H]}{Z[\overline{H}_0+H_V]} = \left\langle \prod_{k=1}^{\infty} \sum_{\mu_k=0}^{\infty} \frac{(x_k)^{\mu_k}}{\mu_k!} \right\rangle_{\text{Gauss}} . \quad (55)$$

If we represent x_k diagrammatically by a ring with k vertices on it (with obvious rules, if we specify that a full line represents $\overline{G}^\sigma_{dd}$), a general term in the series on the rhs of (55) consists of a product of rings. Now the Gaussian averaging may be performed. As a result, all vertices become pairwise connected, and we obtain the same set of diagrams as in an unlinked-diagram expansion for Z with $\overline{H}'$ as a perturbation. [Diagrams with an odd number of vertices in (55) vanish after the averaging.] Since this result is obvious, at least in principle, we do not attempt to present a general proof. Instead of that, we give a specific example, which illustrates the averaging process. The diagram in Fig. 5(a) results from (55) if all μ_k for $k \neq 2$ vanish, but $\mu_2 = 2$. Its contribution C_5 is given by

$$C_5 = \tfrac{1}{8}\Big\langle \sum_{n,\nu,\sigma} (\sigma c/\beta)^2 \overline{G}^\sigma_{dd}(\omega_n)\ \overline{G}^\sigma_{dd}(\omega_{n+\nu}) \times |\xi_\nu|^2 \sum_{m,\lambda,\sigma'} (\sigma' c/\beta)^2 \overline{G}^{\sigma'}_{dd}(\omega_m)\, \overline{G}^{\sigma'}_{dd}(\omega_{m+\lambda}) |\xi_\lambda|^2 \Big\rangle_{\text{Gauss}}$$

$$\equiv \sum_{\lambda,\nu} \langle g_{|\lambda|} |\xi_\lambda|^2 g_{|\nu|} |\xi_\nu|^2 \rangle_{\text{Gauss}} , \quad (56)$$

where it is obvious how $g_{|\lambda|}$ has been defined.

With the aid of

$$\int 2d^2\xi_\nu e^{-2\pi|\xi_\nu|^2} |\xi_\nu|^{2k} = k!/(2\pi)^k , \quad \text{for } \nu \neq 0 \quad (57)$$

$$\int_{-\infty}^{\infty} d\xi_0 e^{-\pi\xi_0^2} \xi_0^{2k} = 1/(2\pi)^k [1\times 3\times 5\times\cdots\times(2k-1)] ,$$

the Gaussian average in (56) can be shown to give

$$(2\pi)^2 C_5 = \sum_{\lambda,\nu} g_{|\lambda|}\, g_{|\nu|} + 2\sum_{\lambda} (g_{|\lambda|})^2 . \quad (58)$$

This result is represented diagrammatically in Fig. 5(b). One can convince oneself easily that the rules (ā) to (ē) from Sec. IV apply. Rule (f̄) turns out to be equivalent to the prescription that one has to sum over the frequencies which are carried by the inter-

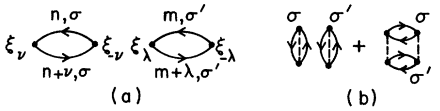

FIG. 5. Two rings in (55), (a) before and (b) after Gaussian averaging.

action lines *after* all other frequencies have been summed over.

Having outlined the relation between the functional-integral representation of $Z[H]$ and the diagrammatic perturbation series in $\bar{H}'$, we turn to a modified perturbation expansion, which is particularly useful for an understanding of the static approximation and the RPA′. We start from expanding $\exp[\sum_\sigma \mathrm{Tr}\ln(1-K^\sigma)]$ in (41) in a multiple power series in $\xi_\nu (\nu \neq 0)$, and take the Gaussian average with respect to all $\nu \neq 0$. We finally obtain

$$Z[H] = Z[\bar{H}_0 + H_V] \int_{-\infty}^{\infty} d\xi_0 Z_{\text{static}}(\xi_0) e^{-\pi\xi_0^2} \exp\tilde{C} \quad . \tag{59}$$

From the derivation of (59) follows that $\tilde{C}$ can be constructed from $\bar{C}$, if we (i) replace $\bar{G}^\sigma_{0\,dd}(\omega_n)$ in $\bar{C}$ by $\tilde{G}^\sigma_{0\,dd}(\omega_n)$, and (ii) observe the condition that only nonzero frequencies can be transferred by the interaction lines. {This follows, of course, from the form of the interaction in K^σ [see (42)].} Comparing this perturbation expansion with the $\bar{H}'$ perturbation series, we arrive at our first result.

Result 1: The static approximation in the functional integral sums those contributions from the $\bar{H}'$ perturbation series which arise from considering only zero-frequency transfer by the interaction lines.

This result is fairly obvious, and can be guessed from similar results obtained in the functional-integral treatment of the BCS Hamiltonian.[11] What is not quite so obvious is the fact that the remaining $\bar{H}'$ perturbation series contributions, which contain zero- and nonzero-frequency interactions, can be summed in such a way that all zero-frequency interactions are represented as a Hartree field in $\tilde{G}^\sigma_{0\,dd}(\omega_n)$. This follows, however, from the physical interpretation of the static approximation. (See Sec. IV and Refs. 1–3.)

Before discussing the drawbacks of the static approximation, we want to gain some insight into the diagrams contributing to $\tilde{C}$.

For that purpose we first sum the "ring diagrams" in Fig. 6. Since a ring diagram with k interaction lines has a symmetry factor $S = 2k$, the series is given by

$$\sum_{k=1}^{\infty} (1/2k) \sum_{\nu\neq 0} [(-c^2/2\pi\beta^2) \sum_{\sigma,n} \tilde{G}^\sigma_n \tilde{G}^\sigma_{n+\nu}]^k$$

$$= -\tfrac{1}{2} \sum_{\nu\neq 0} \ln[1 - (c^2/2\pi) \sum_\sigma \varphi^\sigma_\nu] \quad . \tag{60}$$

Here the definition (51) for φ_ν has been used. Inserting (60) for $\tilde{C}$ in (59) we arrive at the RPA′ approximation (53). This is our second result.

Result 2: The RPA′ approximation in the functional integral corresponds to a ring-diagram summation and the exact treatment of the zero-frequency transfer in the $\bar{H}'$ perturbation series.

There is, however, no criterion that the ring diagrams are the most important diagrams. This may be seen from the other second-order diagrams [in addition to Fig. 5(b)] which have the same topological structure as those drawn in Fig. 1(f) and 1(g). Denoting the contribution of diagrams 5(b), 1(f), 1(g) by X_b, X_f, X_g, respectively, we have

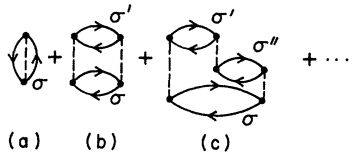

FIG. 6. Ring-diagram approximation for $\tilde{C}$ corresponds to the RPA′ approximation in the functional integral.

$$X_b = \tfrac{1}{4}(c^2/2\pi)^2 \left(\sum_{\nu\neq 0} \sum_\sigma \varphi^\sigma_\nu \right)^2 , \tag{61}$$

$$X_g = -\tfrac{1}{4}(c^2/2\pi)^2 \Big[\sum_{\nu\neq 0} \sum_\sigma (\varphi^\sigma_\nu)^2 - \sum_{n,\nu,\sigma} (1/\beta^4)(\tilde{G}^\sigma_n \tilde{G}^\sigma_\nu)^2 + \sum_{n,\sigma} (1/\beta^4)(\tilde{G}^\sigma_n)^4 \Big], \tag{62}$$

$$X_f = -\tfrac{1}{2}(c^2/2\pi)^2 \Big[\tfrac{1}{4} \sum_{n,\sigma} (\tilde{G}^\sigma_n \sum_\nu \tilde{G}^\sigma_\nu e^{i\omega_\nu\delta} + \tilde{G}^\sigma_n \sum_\nu \tilde{G}^\sigma_\nu e^{-i\omega_\nu\delta})^2 - \sum_{n,\nu,\sigma} (\tilde{G}^\sigma_n)^3 (\tilde{G}^\sigma_\nu e^{i\omega_\nu\delta} + \tilde{G}^\sigma_\nu e^{-i\omega_\nu\delta}) + \sum_{n,\sigma} (\tilde{G}^\sigma_n)^4 \Big]. \tag{63}$$

In calculating these diagrams, we confine ourselves to the symmetric case, without an external magnetic field, and assume $\beta\Gamma \gg 1$.

As a result of the calculations of these sums which are given in the Appendix, we find: (a) The second and third expression in the square brackets in (62) and (63) are negligible compared to the first one. That means for $\beta\Gamma \gg 1$ and $\beta U \gg 1$ we can disregard the restriction to nonzero frequencies in frequency summations. (b) For $c\xi_0 \ll \beta\Gamma$, the contribution X_f is negligible compared to X_b and X_g, while for $c\xi_0$ of the order of c^2 and $\beta\Gamma \gg c^2$, X_f is the most important contribution.

The contributions of higher-order diagrams are much more complicated to write down and to calculate than (61), (62), or (63). Summarizing the results of the calculations (for the third- and some of the fourth-order diagrams), we also find that we can disregard the restriction on nonzero frequencies in frequency summations for $\beta\Gamma \gg 1$ and $\beta U \gg 1$. The diagrams which correspond to X_f are given in Fig. 7. It should be noted that these diagrams *are all of the same order of magnitude for* $c\xi_0 \approx c^2$ *and* $\beta\Gamma \gg c^2$. (This will become clear in Sec. VI.) An immediate consequence of the fact that we have no summation restriction any more in the diagram for $\beta\Gamma \gg 1$ and $\beta U \gg 1$ follows from the considerations in Sec. III.

Result 3: For $\beta\Gamma \gg 1$ and $\beta U \gg 1$, the diagram

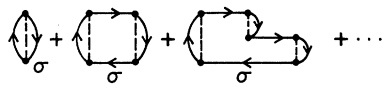

FIG. 7. Most important diagrams for $c\xi_0 \approx c^2$ and $\beta\Gamma \ll c^2$. (Diagrams which result from the above by permuting the two endpoints of an interaction line have been suppressed.)

contributions which result from a pure many-body interaction between equal spins are negligible.

The proof from Sec. III holds equally well if $\bar{G}^{\sigma}_{0\,dd}(\omega_n)$ is replaced by $\tilde{G}^{\sigma}_n$ in all diagrams. Examples of canceling diagrams are the contribution $\frac{1}{2}X_b$[(61)] and X_g[(62)], and it is easy to see that in the RPA′ result (53) φ_ν should be replaced by $\frac{1}{2}\varphi_\nu$ and that we cannot avoid the mathematical breakdown.

In Sec. III we saw further that diagrams with Hartree-Fock self-energies could be renormalized. In Sec. VI we shall apply this concept to the present case. It will be shown that it is crucial to include the series of Fig. 7 in order to get the correct coefficient for Γ/U expansions of physical quantities. We anticipate this result.

Result 4: No finite-order approximation for the fluctuations in the functional integral can lead to the correct coefficients in the Γ/U expansion of physical quantities. This result holds true in particular for the static approximation and the RPA′. We also understand why the static approximation does not correctly give the first-order coefficient in the U/Γ expansion: In the static approximation diagram 6(a) is not included. Since it is included in RPA′, this approximation gives the U/Γ coefficient correctly.

Reviewing the main outcome of this section, we wish to emphasize that the application of functional-integral methods to the Hamiltonian (6) leads into difficulties, since the possible approximations in the functional integral sum only a part of the artificially introduced many-body interaction between equal spins (see result 4).

We conclude this section with sketching another simple example of this fact. Writing H_0+H_V [from (2) and (4)] as

$$H_0+H_V=\sum_{\vec{k}\sigma}\epsilon_{\vec{k}\sigma}c^{\dagger}_{\vec{k}\sigma}c_{\vec{k}\sigma}+\sum_{\sigma}\epsilon_d c^{\dagger}_{d\sigma}c_{d\sigma}$$
$$-\sum_{\sigma}\sigma g'\mu B c^{\dagger}_{d\sigma}c_{d\sigma}c^{\dagger}_{d\sigma}c_{d\sigma}+H_V, \qquad (64)$$

We have artificially introduced a two-particle interaction in an exactly soluble model. Applying functional-integral methods to (64), we find that the static approximation leads to correct limits $B=0$ and $H_V=0$. The RPA′ approximation, however, breaks down mathematically. This example illustrates clearly that the known approximations in the functional integral are insufficient. We therefore turn to establishing a combined perturbation-technical and functional-integral approach.

VI. RENORMALIZED APPROXIMATIONS IN FUNCTIONAL INTEGRAL

In principle, Eq. (59) provides us with a tool to combine the advantages of the functional-integral method with perturbation expansions. While ordinary perturbation expansions necessarily are restricted in their validity to *one* of the two limits of the Anderson model, the static approximation is valid in *both* limits. We can easily improve the static approximation in approximating $\tilde{C}$ in (59) by including all diagrams up to a certain power in $c^2/2\pi=\beta U$. This approximation, however, is a systematic one only in the small U/Γ case. There is no guarantee that it is valid in the large U/Γ case on which we want to concentrate our effort in this section.

We start from the observation that in that case the integrand in (59) has two sharp maxima near $|\xi_0|=c/2\pi$, provided that $\exp\tilde{C}$ behaves reasonably as a function of ξ_0. So we may judge the contribution of a diagram in the large U/Γ case from its behavior near $|\xi_0|=c/2\pi$. For $\xi_0 \sim c$, we have already seen that among the second-order diagrams only the one drawn in Fig. 7 with the contribution X_f from (63) has to be taken into account. The second-order ring-diagram contribution, on the other hand, is negligible. [One can easily convince oneself that from the ring-diagram series in (60) only the first term contributes appreciably for $\xi_0 \sim c$.]

The most important diagrams in every order are given by the series drawn in Fig. 7. It was stated in Sec. V that they all are of the same order of magnitude. Indeed, for the first-order diagram we have the contribution

$$-\tfrac{1}{2}(c^2/2\pi)(1/\beta^2)\sum_{\sigma,n,\nu\neq 0}\tilde{G}^{\sigma}_n\tilde{G}^{\sigma}_{n+\nu}$$
$$=(c^2/2\pi)\{\tfrac{1}{4}-[(1/\pi)\arctan(c\xi_0/\beta\Gamma)]^2-(1/2\pi)\beta\Gamma/$$
$$[(\beta\Gamma)^2+(c\xi_0)^2]\}. \qquad (65)$$

Here we have evaluated the sums over n and ν with the aid of rule (f) of Sec. III and have restricted ourselves to the symmetric case in zero magnetic field and $\beta\Gamma \gg 1$. The general expression can be written down from the Appendix [Eq. (A3)]. The last term in the curly bracket results from the $\nu=0$ contribution in the sum, and one can convince oneself quite easily that it can be neglected if $\beta\Gamma \gg 1$, in particular near the maximum $(c\xi_0)^2=c^4/(2\pi)^2$, where the diagram has a contribution of the order of $\beta\Gamma/c\xi_0$.

The contribution of the kth-order diagram of the series in Fig. 7 ($k \geq 2$) is given by

$$-1/k(c^2/2\pi\beta^2)^k\sum_{\sigma,n}(\tilde{G}^\sigma_n\sum_{\nu\neq 0}{}'\tilde{G}^\sigma_{n+\nu})^k$$

$$\approx -(1/k)(c^2/2\pi\beta^2)^k\sum_{\sigma,n}[\tilde{G}^\sigma_n(\sigma/\pi)\arctan(c\xi_0/\beta\Gamma)]^k. \tag{66}$$

Here $1/k$ is the reciprocal symmetry factor of the diagram, and the prime on the first sum denotes a principal value. The right-hand side again holds true for $\beta\Gamma\gg 1$, no-magnetic-field, symmetric case. Near the maximum, the arctan in (66) may be replaced by $\frac{1}{2}\pi$, and the remaining n sum is given by the kth derivative with respect to $c\xi_0$ of the expression given in (A4). So we obtain for (66) an order of magnitude of $\beta\Gamma/c\xi_0$, near the maximum, and thus there the whole series drawn in Fig. 7 is of importance.

From (65) and (66) we find for the total contribution of the diagrams in Fig. 7:

$$\frac{c^2}{8\pi}+\frac{c^2}{2\pi^3}\arctan\left(\frac{c\xi_0}{\beta\Gamma}\right)^2-\sum_{k=1}^{\infty}\frac{1}{k}\left(\frac{c^2}{2\pi\beta^2}\right)^k$$

$$\times\sum_{\sigma,n}e^{i\omega_n\delta}\left(\tilde{G}^\sigma_n\frac{\sigma}{\pi}\arctan\frac{c\xi_0}{\beta\Gamma}\right)^k$$

$$=\frac{c^2}{2\pi}\left[\frac{1}{4}+\left(\frac{1}{\pi}\arctan\frac{c\xi_0}{\beta\Gamma}\right)^2\right]-\frac{2c|\xi_0|}{\pi}\arctan\left(\frac{c|\xi_0|}{\beta\Gamma}\right)$$

$$+\frac{2c|\xi_0|-2|A|}{\pi}\arctan\left(\frac{c|\xi_0|-|A|}{\beta\Gamma}\right)$$

$$-\frac{\beta\Gamma}{\pi}\ln\left[1+\frac{-2|A||\xi_0|c+|A|^2}{(\beta\Gamma)^2+(c\xi_0)^2}\right], \tag{67}$$

with

$$A=(c^2/2\pi^2)\arctan(c\xi_0/\beta\Gamma). \tag{68}$$

We want to stress that (67) is a valid expression only near the maxima. Only there it represents an improvement over the static approximation, which may be seen from the fact that we obtain the correct expression for the susceptibility from approximating $\tilde{C}$ in (59) by (67). The susceptibility is given by[1]

$$\chi=\chi_{\text{Band}}-\frac{1}{U}\left(\frac{g}{2}\mu_B\right)^2\left[1+2\frac{\partial}{\partial\gamma}\ln Z(\gamma)\right]_{\gamma=1}, \tag{69}$$

where

$$Z(\gamma)=Z[\bar{H}_0+H_V]\int_{-\infty}^{\infty}d\xi_0 e^{-\pi\gamma\xi_0^2}Z_{\text{static}}(\xi_0)\exp\tilde{C}. \tag{70}$$

Inserting (67) for $\tilde{C}$, the integrand of (70) near the maxima $\xi_0=c/2\pi\gamma$ is approximated by

$$\exp\{-\pi\gamma\xi_0^2+c|\xi_0|-(2/\pi)\beta\Gamma-(\beta\Gamma/\pi)$$

$$\times\ln[1+(c|\xi_0|-|A|)^2/\beta\Gamma]\}.$$

The saddle-point integration yields

$$\ln Z(\gamma)=\text{const}-\tfrac{1}{2}\ln\gamma+\frac{c^2}{4\pi\gamma}-\frac{2\beta\Gamma}{\pi}\ln\left(\frac{1}{2\pi\gamma}-\frac{1}{4\pi}\right), \tag{71}$$

$$2\frac{\partial\ln Z(\gamma)}{\partial\gamma}\bigg|_{\gamma=1}=-1-\frac{c^2}{2\pi}+\frac{8\beta\Gamma}{\pi}, \tag{72}$$

whereupon

$$\chi=\chi_{\text{Band}}+\frac{1}{kT}\left(\frac{g}{2}\mu_B\right)^2\left(1-\frac{8\Gamma}{\pi U}\right) \tag{73}$$

follows, in agreement with, e.g., Scalapino.[16]

Consequently, our plan of summing the most important diagrams near the maxima has led to the correct result for the susceptibility up to Γ/U in the local-moment limit and (obviously, since the first-order diagram in U is included) to the correct result up to U/Γ in the Pauli-susceptibility limit.

We next make use of result 3 of Sec. V for $\beta\Gamma\gg 1$ and $\beta U\gg 1$. Then in analogy to Sec. III, the only interaction between equal spins which remains for $\beta\Gamma\gg 1$ and $\beta U\gg 1$ is represented by the exchange contribution of the Hartree-Fock self-energy in the Green's-function lines. (The direct or Hartree term is already included in the static approximation.) As in (27), we renormalize the Green's function $\tilde{G}^\sigma$ in all genuine many-body diagrams by this self-energy and obtain

$$\tilde{G}^\sigma_n[1-(1/\beta)\tilde{G}^\sigma_n(c^2/2\pi)\textstyle\sum_\nu{}'\tilde{G}^\sigma_{n+\nu}]^{-1}\equiv\tilde{\tilde{G}}^\sigma_n$$

$$=\{i\omega_n-\bar{\epsilon}_{d\sigma}+(1/\beta)[\sigma c\xi_0-(c^2/2\pi^2)$$

$$\times\arctan(-\beta\bar{\epsilon}_{d\sigma}+\sigma c\xi_0)/\beta\Gamma]-S^\sigma(\omega_n)\}^{-1}, \tag{74}$$

while the sum of the diagrams which contain nothing but the exchange term of the Hartree-Fock self-energy as an interaction represents a correction to the static partition function and has been calculated in (67).

Near the maxima of the integrand in (59) $\sigma\xi_0=c/2\pi$, the new Green's function $\tilde{\tilde{G}}^\sigma_n$ resembles the Green's function $G^\sigma_{0dd}(\omega_n)$ in (24). We have achieved there the major goal of renormalizing the d-electron energies to their original value (3) in the large U limit and have gotten rid of the artificially introduced many-body interaction.

Our final version of the functional integral in the one-variable scheme, valid for $\beta\Gamma\gg 1$ and $\beta U\gg 1$, reads

$$Z[H]=Z[\bar{H}_0+H_v]\int_{-\infty}^{\infty}d\xi_0 Z^{\text{ren}}_{\text{stat}}(\xi_0)e^{-\pi\xi_0^2}\exp\tilde{\tilde{C}}. \tag{75}$$

Here $Z^{\text{ren}}_{\text{static}}$ is the product of $Z_{\text{static}}(\xi_0)$ and the rhs of (67). $\tilde{\tilde{C}}$ is given by topologically the same set of diagrams as C in Sec. III but without Hartree-type self-energy inclusion in the Green's-function lines, which represent $\tilde{\tilde{G}}^\sigma_n$, as given in

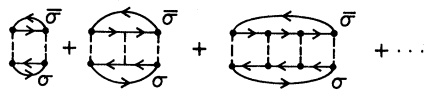

FIG. 8. Particle-hole ladder series which leads to the Kondo effect.

(74). In Sec. VII we shall start from (75) and calculate the first Kondo $\ln(T/D)$ term for the susceptibility.

VII. KONDO EFFECT

The Schrieffer-Wolff transformation,[23] which connects the Anderson model with the Kondo model, first led to the conclusion that the susceptibility of the Anderson model shows a logarithmic temperature dependence in the $(\Gamma/U)^2$ coefficient. This result was later confirmed by Scalapino[16] and in more detail by Dworin.[24] We shall see later that in order to find this result, we are not allowed to approximate $S^\sigma(\omega_n)$ from (16) by a constant level width as in (17). Consequently, the susceptibility formula (69) is not valid for the Kondo regime, and we have to start from the partition function in an external magnetic field. As a guide for finding the Kondo term, we can use the fact that for zero magnetic field there is no anomalous temperature dependence in the $(\Gamma/U)^2$ coefficient. Consequently, we have to look for a singularity in the diagrams which vanishes for zero magnetic field. Physical intuition suggests to expect this singularity in an infinite series of diagrams and not in a single diagram. Such a singularity indeed occurs in the particle-hole-ladder series, drawn in Fig. 8. (The particle and the hole have opposite spin.) The symmetry factor of a kth-order diagram is $S=2k$. Denoting the sum in Fig. 8 by L, we have for $\beta\Gamma\gg 1$, $\beta U\gg 1$, and a finite ratio Γ/U,

$$L\approx -\tfrac{1}{2}\sum_{\sigma,\nu}\ln[1+(c^2/2\pi\beta^2)\sum_n \tilde{\tilde{G}}^{\sigma}_{n+\nu}\tilde{\tilde{G}}^{\bar{\sigma}}_{n}] + \tfrac{1}{2}\sum_{\sigma,\nu}(c^2/2\pi\beta^2)\sum_n \tilde{\tilde{G}}^{\sigma}_{n+\nu}\tilde{\tilde{G}}^{\bar{\sigma}}_{n}\ . \tag{76}$$

Approximating $\tilde{C}$ in (75) by the particle-hole ladder series L, we look for contributions to the grand partition function, which come from the $(\Gamma/U)^2$ expansion of L.

We want to emphasize however that (76) is not valid for $\Gamma/U=0$. As we know from the static approximation, for $\Gamma/U=0$ only the zero-frequency transfer is important and all $\tilde{C}$ or $\tilde{\tilde{C}}$ diagrams have to vanish. One can check this easily for an arbitrary diagram for L, taking explicitly into account the summation restrictions on nonzero frequencies. It turns out that L vanishes even up to the first power in Γ/U. [For the first diagram of L we know this result already from (61) and (A6).] Expanding up to second order, we may discriminate between contributions coming from expanding only Green's-function lines carrying the same spin (i.e., belonging to the upper or the lower closed electron line in an L diagram) and those coming from two Green's-function lines with opposite spins. In the former case, we again get no contribution.

Instead of drawing all the conclusions from diagrams, we could have examined the exact expression for the particle-hole ladder series L while taking explicitly into account the zero-frequency summation restrictions. It is given by

$$L=\int_0^1 \frac{d\lambda}{2\lambda}\sum_{\sigma,\nu}\frac{1}{1-x}\left[x^2+U_0^2\frac{\partial}{\partial U_0}\left(\frac{1}{U_0}\,x\right)\right], \tag{77}$$

where

$$U_0=-\lambda c^2/2\pi\ , \tag{78}$$

$$x=U_0\textstyle\sum_n[U_0+\beta^2(\tilde{\tilde{G}}^{\sigma}_{n+\nu}\tilde{\tilde{G}}^{-\sigma}_{n})^{-1}]^{-1}. \tag{79}$$

The terms resulting from two Green's-function lines with opposite spins can either come from expanding (79) up to second order in Γ or from expanding two different x up to first order in Γ. The former contributions, which we denote by $L_1^{(4)}$, come from the particle-hole pair between two subsequent rungs. The latter contributions will be denoted by $L_2^{(4)}$.

We first concentrate on the calculation of $L_1^{(4)}$. In view of the fact that $\infty\gg\beta U\gg\beta\Gamma\gg 1$, we may calculate $L_1^{(4)}$ from (76), which is much simpler than (77). We then have from (75)

$$Z_1^{(4)}\to Z[\bar{H}_0]\int_{-\infty}^{\infty}d\xi_0 e^{-\pi\xi_0^2}\,Z^{\rm ren}_{\rm static}(\xi_0)\big|_{\Gamma/U=0}L_1^{(4)}\ . \tag{80}$$

Denoting the particle-hole propagator by P_ν,

$$P_\nu=(c^2/2\pi\beta^2)\textstyle\sum_n\tilde{\tilde{G}}^{\sigma}_{n+\nu}\tilde{\tilde{G}}^{-\sigma}_{n}, \tag{81}$$

we obtain

$$L_1^{(4)}=-\tfrac{1}{2}\sum_{\sigma,\nu}\left(\frac{1}{1+P_\nu}\bigg|_{\Gamma/u=0}-1\right)P_\nu^{(4)}\ , \tag{82}$$

with

$$P_\nu^{(4)}=\frac{c^2}{2\pi\beta^2}\sum_n(\tilde{\tilde{G}}^{\sigma}_{n+\nu}\tilde{\tilde{G}}^{-\sigma}_{n})^2{}_{\Gamma/U=0}\times\left(\sum_k|V_{kd}|^2\frac{1}{i\omega_{n+\nu}-\epsilon_{k\sigma}}\right)\times\left(\sum_{k'}|V_{k'd}|^2\frac{1}{i\omega_n-\epsilon_{k'\bar{\sigma}}}\right)\ . \tag{83}$$

For $\Gamma/U=0$, the renormalized static expression $Z^{\rm ren}_{\rm static}(\xi_0)$ has to go over to the static result $Z_{\rm static}(\xi_0)$, since the correction term (67) holds true only

near $|\xi_0| = c/2\pi$. In evaluating the integral in (80), we then can apply the saddle-point integration method and evaluate $L_1^{(4)}$ near $\xi_0 = \pm c/2\pi$.

Restricting again to the symmetric case, we first calculate $P_\nu|_{\Gamma/U=0}$. With $s = \xi_0/|\xi_0|$, we obtain

$$P_\nu|_{\Gamma/U=0,\, t_0=sc/2\pi} = \frac{c^2}{2\pi\beta^2}\sum_n \frac{1}{(i\omega_{n+\nu}+\sigma s\, c^2/4\pi\beta+\sigma g'\,\mu B)(i\omega_n-\sigma s\, c^2/4\pi\beta-\sigma g'\,\mu B)}$$

$$= \frac{c^2}{2\pi}\,\frac{f(\sigma s c^2/4\pi\beta+\sigma g'\,\mu B)-f(-\sigma s\, c^2/4\pi\beta-\sigma g'\,\mu B)}{2\pi i\,\nu+\sigma s\, c^2/2\pi+2\sigma\beta g'\,\mu B} = \frac{c^2}{2\pi}\,\frac{-\sigma s}{2\pi i\,\nu+\sigma s\, c^2/2\pi+2\sigma\beta g'\,\mu B}\quad . \tag{84}$$

Here we have expressed $\epsilon_{d\sigma}$ according to (3) and have replaced the Fermi functions by ± 1 because of $c^2/2\pi \gg 1$.

From (84) it follows that

$$-\frac{1}{2}\left(\frac{1}{1+P_\nu}-1\right)_{\Gamma/U=0} = -\frac{1}{2}\left[\left(1+\frac{-\sigma s\, c^2/2\pi}{2\pi i\,\nu+\sigma s\, c^2/2\pi+2\sigma\beta g'\,\mu B}\right)^{-1}-1\right] = -\frac{1}{2}\left(\frac{c^2}{2\pi}\right)\frac{\sigma s}{2\pi i\,\nu+2\sigma\beta g'\,\mu B}\quad . \tag{85}$$

The behavior of this expression in the limits $\nu \to 0$ and $B \to 0$ obviously depends on the order in which these limits are taken.

We next insert (85) into (82) and calculate (80) by saddle-point integration. We obtain

$$Z_1^{(4)}[H] \to Z_{\text{Band}}\, e^{c^2/4\pi}\sum_{s=\pm1}\sum_\nu e^{s\beta g'\mu B}\left(-\frac{1}{2}\right)\frac{c^2}{2\pi}\,\frac{\sigma s}{2\pi i\,\nu+2\sigma\beta g'\,\mu B}\,P_\nu^{(4)}|_{t_0=sc/2\pi}\quad . \tag{86}$$

With $P_1^{(4)}$ from (83), (86) becomes

$$Z_1^{(4)}[H] \to Z_{\text{Band}}\, e^{\beta U/2}\sum_{s=\pm1} e^{s\beta g'\mu B}\left(-\frac{1}{2}\right)U^2[\sigma s/(2\pi i\,\nu+2\sigma\beta g'\,\mu B)]\sum_{\vec{k},\vec{k}',n,\nu}[i\omega_{n+\nu}+\sigma(s\tfrac{1}{2}U+g'\,\mu B)]^{-2}$$

$$\times[i\omega_n-\sigma(s\tfrac{1}{2}U+g'\,\mu B)]^{-2}\,|V_{\vec{k}d}|^2\,|V_{\vec{k}'d}|^2[(i\omega_{n+\nu}-\epsilon_{\vec{k}\sigma})(i\omega_n-\epsilon_{\vec{k}'\bar{\sigma}})]^{-1}\quad . \tag{87}$$

The σ sum in (87) simply yields a factor of 2. The n sum can be done by contour integration, whereupon the main contribution to (87) will come from the two first-order poles at $2\pi i\,\nu/\beta-\epsilon_{\vec{k}\sigma}$ and at $\epsilon_{\vec{k}'\sigma}$. Replacing the squared denominators by appropriate averages, we then obtain

$$Z_1^{(4)}[H] \to Z_{\text{Band}}\, e^{\beta U/2}\sum_{s=\pm1,\,\nu} e^{s\beta g'\mu B}(-1)\,\frac{16}{U^2}\,\frac{\beta s}{2\pi i\nu+2\beta g'\,\mu B}\sum_{k,k'}|V_{kd}|^2\,|V_{k'd}|^2\,\frac{f(\epsilon_{\vec{k}\uparrow})-f(\epsilon_{\vec{k}'\downarrow})}{2\pi i\,\nu/\beta-\epsilon_{\vec{k}\uparrow}+\epsilon_{\vec{k}'\downarrow}}\quad . \tag{88}$$

The ν sum finally gives cotanh functions of the energy denominators, and after some rearrangement, (88) can be written

$$Z_1^{(4)}[H] \to Z_{\text{Band}}\, e^{\beta U/2}\left[\sum_{s=\pm1} e^{s\beta g'\mu B}\left(\frac{-8\beta s}{U^2}\right)\sum_{\vec{k}\vec{k}'}|V_{\vec{k}d}|^2\,|V_{\vec{k}'d}|^2\,\frac{(1-f_{\vec{k}\uparrow})f_{\vec{k}'\downarrow}+f_{\vec{k}\uparrow}(1-f_{\vec{k}'\downarrow})}{2g'\,\mu B-\epsilon_{\vec{k}'\downarrow}+\epsilon_{\vec{k}\uparrow}}\right.$$

$$\left.+\sum_{\vec{k}\vec{k}'}|V_{\vec{k}d}|^2\,|V_{\vec{k}'d}|^2\,\frac{(-8\beta)}{U^2}\,\frac{f_{\vec{k}\uparrow}-f_{\vec{k}'\downarrow}}{2g'\,\mu B-\epsilon_{\vec{k}'\downarrow}+\epsilon_{\vec{k}\uparrow}}\,(e^{\beta g'\mu B}+e^{-\beta g'\mu B})\right]\quad . \tag{89}$$

One easily sees that the rhs of (89) is an even function of the magnetic field and that the first nonvanishing contribution of the first term shows a logarithmic singularity. Using the definition (17) for Γ, we obtain

$$Z_1^{(4)}[H] \to Z_{\text{Band}}\, e^{\beta U/2}\,\frac{64gg'(\beta\mu B)^2}{\pi^2}\left(\frac{\Gamma}{U}\right)^2\ln\left(\frac{T}{D}\right)\quad . \tag{90}$$

Here D is of the order of the bandwidth.

Multiplying this expression by $(-1/\beta)$, we obtain the corresponding correction for the free energy, from which the susceptibility follows in agreement with Scalapino.[16]

From the above analysis it is clear that the contribution of $L_2^{(4)}$ does not lead to a Kondo-type singularity. An explicit calculation, however, is difficult, for we cannot use (76) anymore. The second derivative with respect to $c^2/2\pi\beta^2$ of (76) develops an unphysical singularity at $\Gamma/U = 0$, since the condition Γ/U = finite is hurt. Consequently we have to consider the exact expression (77) or we have to examine the diagrams. It is not difficult to see that in the diagrams a combination of denominators like in (88) never occurs, if we look for the $(\Gamma/U)^2$ expansion of a pair of Green's functions of opposite spin, which do not belong to a particle-hole pair between two subsequent rungs.

VIII. CONCLUSION

In Sec. VII we saw the Kondo effect resulting from a singularity in the particle-hole propagation. We calculated only in the small Γ/U limit, though the approximation is valid also in the U/Γ limit and gives the $(U/\Gamma)^2$ coefficients of physical quantities correctly, as is clear from the foregoing. An analytical evaluation of the sum (77), however, is impossible. Consequently, we cannot answer the question how the Kondo effect vanishes for $U\sim\Gamma$. Furthermore, it is not clear whether the particle-hole ladder is important at all in the intermediate region $U\sim\Gamma$. It is our feeling from the analysis of this paper that all diagrams are of equal importance in that region. In order to find a reasonable approximation, one has no reliable guide like perturbation theory. There the only possibility seems to be to establish self-consistent approximations using the results of Sec. III, Eqs. (32) and (33). Technically this is extremely complicated. It is clear that all these improvements over the static approximation cannot be obtained by applying the conventional functional-integral methods of distinguishing certain frequencies or restricting to Gaussian fluctuations. In addition, we have seen that there is a nontrivial renormalization problem in the one-variable functional-integral approach, because one starts from a Hamiltonian, where the d-electron energy is shifted.

Altogether, it must be said that the conventional functional-integral approach to the Anderson model does not seem to be technically easier than other many-body methods.

ACKNOWLEDGMENTS

The author wishes to thank Professor J. R. Schrieffer, Dr. W. E. Evenson, and S. Q. Wang for many stimulating discussions of their work. He is especially grateful to Professor J. R. Schrieffer for his discussions during the work and his criticism and advice concerning the manuscript, and to Dr. W. E. Evenson for a very careful reading of the manuscript and suggestions. He would also like to thank the Deutsche Forschungsgemeinschaft for financing his stay in the United States.

APPENDIX

Here we calculate several frequency sums which are needed in the main text.

(a) We begin with

$$\frac{1}{\beta}\sum_{\omega_n} e^{i\omega_n\delta}\frac{1}{i\omega_n+i\Gamma\,\mathrm{sign}\omega_n}=\frac{1}{2\pi}\int_{-\infty}^{\infty}d\omega f(\omega)\,\frac{2\Gamma}{\omega^2+\Gamma^2}$$

$$=\frac{1}{4\pi}\int_{-\infty}^{\infty}d\omega\,[f(\omega)+f(-\omega)]\,\frac{2\Gamma}{\omega^2+\Gamma^2}=\frac{1}{2\pi}\int_{-\infty}^{\infty}d\omega\,\frac{\Gamma}{\omega^2+\Gamma^2}=\frac{1}{2}\,. \tag{A1}$$

Here the first step follows from converting the sum in the usual way into an integral with the Fermi function $f(\omega)$, and exploiting the analytic properties of the integrand. In the same way we find

$$\frac{1}{\beta}\sum_{\omega_n} e^{-i\omega_n\delta}\frac{1}{i\omega_n+i\Gamma\,\mathrm{sign}\omega_n}=-\frac{1}{2}\,. \tag{A2}$$

(b) With $\tilde{G}_n^\sigma$ from (43) and (17), and with the aid of (A1), we have

$$\frac{1}{\beta}\sum_{\omega_n} e^{i\omega_n\delta}\tilde{G}_n^\delta=\sum_n\left[\frac{1}{i\beta\omega_n-\beta\bar{\epsilon}_{d\sigma}+\sigma c\xi_0+i\beta\Gamma\,\mathrm{sign}\omega_n}-\frac{1}{i\beta\omega_n+i\beta\Gamma\,\mathrm{sign}\omega_n}\right]+\frac{1}{2}$$

$$=\frac{1}{\pi}\,\mathrm{Im}\left\{\sum_{n\geq 0}\left[\frac{-1}{n+\frac{1}{2}+(i/2\pi)(-\beta\bar{\epsilon}_{d\sigma}+\sigma c\xi_0)+\beta\Gamma/2\pi}+\frac{1}{n+\frac{1}{2}+\beta\Gamma/2\pi}\right]\right\}+\frac{1}{2}\,.$$

Here we were allowed to neglect the exponential factor in front of the square bracket since the corresponding sum converges. The sum on the non-negative n's is a well-known representation of digamma functions.[25] Consequently, we have

$$(1/\beta)\sum_{\omega_n} e^{\pm i\omega_n\delta}\tilde{G}_n^\sigma=\pm\tfrac{1}{2}+(1/\pi)\,\mathrm{Im}\psi[\tfrac{1}{2}+\beta\Gamma/2\pi+(i/2\pi)(-\beta\bar{\epsilon}_{d\sigma}+\sigma c\xi_0)]\,. \tag{A3}$$

It is easy to find the following limiting cases of (A3):

$$\frac{1}{\beta}\sum_{\omega_n} e^{\pm i\omega_n\delta}\tilde{G}_n^\sigma=\pm\tfrac{1}{2}+(1/\pi)\arctan[(-\beta\bar{\epsilon}_{d\sigma}+\sigma c\xi_0)/\beta\Gamma]\,,\quad \text{for } \beta\Gamma\gg 1$$

$$=\pm\tfrac{1}{2}+\tfrac{1}{2}\tanh[\tfrac{1}{2}(-\beta\bar{\epsilon}_{d\sigma}+\sigma c\xi_0]\,,\qquad \text{for } \beta\Gamma=0\,. \tag{A4}$$

(c) Next we calculate the sum occurring in the static partition function (40):

$$\sum_{\sigma,n} e^{i\omega_n\delta}\ln[1+(\sigma c/\beta)\xi_0\bar{G}^{\sigma}_{0dd}(\omega_n)]=\sum_{\sigma}\int_0^c d\gamma\,\frac{\partial}{\partial\gamma}\sum_n e^{i\omega_n\delta}\ln\left[1+\frac{\sigma\gamma}{\beta}\,\xi_0\bar{G}^{\sigma}_{0dd}(\omega_n)\right]$$

$$=\sum_{\sigma,n}\int_0^c d\gamma\, e^{i\omega_n\delta}\,\frac{(1/\beta)\sigma\xi_0}{[\bar{G}^{\sigma}_{0dd}(\omega_n)]^{-1}+\sigma\gamma\xi_0/\beta}$$

$$=\sum_{\sigma,n}(\sigma\xi_0/\beta)\int_0^c d\gamma\, e^{i\omega_n\delta}\,\tilde{G}^{\sigma}_n(c-\gamma)$$

$$=\sum_{\sigma}\sigma\xi_0\int_0^c d\gamma\{\tfrac{1}{12}+(1/\pi)\mathrm{Im}\psi[\tfrac{1}{2}+\beta\Gamma/2\pi+(i/2\pi)(-\beta\bar{\epsilon}_{d\sigma}+\sigma\gamma\xi_0)]\}$$

$$=-2\sum_{\sigma}\ln\left|\frac{\bar{\Gamma}(\frac{1}{2}+\beta\Gamma/2\pi-(i/2\pi)(\beta\bar{\epsilon}_{d\sigma}-\sigma c\xi_0))}{\bar{\Gamma}(\frac{1}{2}+\beta\Gamma/2\pi-(i/2\pi)\beta\bar{\epsilon}_{d\sigma})}\right|\,. \tag{A5}$$

The last line follows from the definition of the ψ function as logarithmic derivative of the Γ function (here called $\bar{\Gamma}$ to distinguish it from the quantity Γ). The limiting case $\beta\Gamma\gg 1$ of (A5) is given in (47) and is in agreement with Eq. (8) of Ref. 1.

(d) We calculate φ^{σ}_{ν} from Eq. (51). Since φ^{σ}_{ν} is an even function in ν, we may assume $\nu>0$. We then split the n sum into three parts $n\geq 0$, $0>n\geq-\nu$, $-\nu>n>-\infty$. Any of them can be expressed in terms of digamma functions. Writing for short $a=(1/2\pi i)(-\beta\bar{\epsilon}_{d\sigma}+\sigma c\xi_0)$, we have

$$\varphi^{\sigma}_{\nu}=\frac{-1}{(2\pi)^2}\,\frac{2}{\nu}\,\mathrm{Re}\left[\psi\left(\frac{1}{2}+\frac{\beta\Gamma}{2\pi}+a\right)+\psi\left(\frac{1}{2}+\frac{\beta\Gamma}{2\pi}+\nu+a\right)\right]-\frac{1}{(2\pi)^2}\,\frac{1}{\nu+\beta\Gamma/\pi}\left[\psi\left(-\nu+\frac{1}{2}+a-\frac{\beta\Gamma}{2\pi}\right)\right.$$

$$\left.+\psi\left(\nu+\frac{1}{2}+a+\frac{\beta\Gamma}{2\pi}\right)-\psi\left(\frac{1}{2}+\frac{\beta\Gamma}{2\pi}+a\right)-\psi\left(\frac{1}{2}-\frac{\beta\Gamma}{2\pi}+a\right)\right]. \tag{A6}$$

For $\beta\Gamma=0$ we have $\varphi^{\sigma}_{\nu}=0$, and for $\beta\Gamma\gg 1$ we obtain Eq. (52).

(e) The sum (61), which we want to calculate next, can only be estimated. We have for $\beta\Gamma\gg 1$, $\bar{\epsilon}_{d\sigma}=0$ from (61) and (52)

$$X_b=\left(\frac{c^2}{2\pi}\right)^2 2\left(\frac{\beta\Gamma}{2\pi}\right)^2\sum_{\nu>0}\left\{\frac{1}{\Omega_\nu(\Omega_\nu+2\beta\Gamma)}\ln\left[1+\frac{\Omega_\nu(\Omega_\nu+2\beta\Gamma)}{\beta^2\Gamma^2+c^2\xi_0^2}\right]\right\}^2.$$

Using the inequality (for $\alpha x>0$) $\alpha x/(1+\alpha x)\leq\ln(1+\alpha x)\leq\alpha x$, we obtain

$$2\left(\frac{c^2}{2\pi}\right)^2\left(\frac{\beta\Gamma}{\pi}\right)^2(\beta^2\Gamma^2+c^2\xi_0^2)^{-2}\sum_{\nu>0}\left(1+\frac{\Omega_\nu(\Omega_\nu+2\beta\Gamma)}{\beta^2\Gamma^2+c^2\xi_0^2}\right)^{-2}$$

$$\leq X_b\leq\frac{\beta\Gamma}{\pi}\left(\frac{c^2}{2\pi}\right)^2\frac{1}{\beta^2\Gamma^2+c^2\xi_0^2}\;2\sum_{\nu>0}\frac{\beta\Gamma}{\pi\Omega_\nu(\Omega_\nu+2\beta\Gamma)}\ln\left(1+\frac{\Omega_\nu(\Omega_\nu+2\beta\Gamma)}{\beta^2\Gamma^2+c^2\xi_0^2}\right).$$

All sums can be represented by digamma functions, which subsequently are replaced by their asymptotic series. We finally obtain

$$\left(\frac{c^2}{2\pi}\right)^2\left(\frac{\beta\Gamma}{c\xi_0}\right)^2\frac{1}{2\pi^3}\left(\frac{1}{c\xi_0}\arctan\frac{c\xi_0}{\beta\Gamma}-\frac{\beta\Gamma}{\beta^2\Gamma^2+c^2\xi_0^2}\right)\leq X_b\leq\left(\frac{c^2}{2\pi}\right)^2\frac{\beta\Gamma}{\pi}\frac{1}{\beta^2\Gamma^2+c^2\xi_0^2}\left[\frac{1}{4}-\frac{1}{\pi^2}\left(\arctan\frac{c\xi_0}{\beta\Gamma}\right)^2\right]. \tag{A7}$$

For $c\xi_0\ll\beta\Gamma$, the inequality reads

$$\frac{1}{3\pi^3}\left(\frac{c^2}{2\pi}\right)^2\frac{1}{\beta\Gamma}\leq X_b\leq\left(\frac{c^2}{2\pi}\right)^2\frac{1}{4\pi\beta\Gamma},$$

and X_b is of the order of $c^4/\beta\Gamma$ for $c\xi_0\ll\beta\Gamma$. For $c\xi_0\gg\beta\Gamma$, the inequality reads

$$\left(\frac{c^2}{2\pi}\right)^2\frac{(\beta\Gamma)^2}{|c\xi_0|^3}\frac{1}{4\pi^2}\leq X_b\leq\left(\frac{c^2}{2\pi}\right)^2\frac{\beta^2\Gamma^2}{\pi^2|c\xi_0|^3},$$

and X_b is of the order of $(\beta\Gamma/\xi_0)^2$ near $c\sim\xi_0$ and $c\xi_0\gg\beta\Gamma$.

(f) The calculation of X_g from (62) is quite easy. Since the first term on the rhs of (62) is $-\frac{1}{2}X_b$, the same estimates as in (A7) hold. The second and the third term on the rhs of (62) can be easily obtained by differentiation from (A4). Finally we obtain

$$X_g=-\tfrac{1}{2}X_b+\left(\frac{c^2}{2\pi}\right)^2\left\{\frac{1}{2\pi^2}\left(\frac{\beta\Gamma}{\beta^2\Gamma^2+c^2\xi_0^2}\right)^2\right.$$

$$\left.-\frac{1}{12\pi}\frac{\beta\Gamma}{(\beta^2\Gamma^2+c^2\xi_0^2)^2}\left[-1+\frac{2c^2\xi_0^2}{(\beta\Gamma)^2+c^2\xi_0^2}\right]\right\}, \tag{A8}$$

and it is clear that the curly bracket in (A8) is one order of magnitude smaller than the leading terms, provided that $\beta\Gamma \gg 1$. Using (A4), the calculation of X_f in (63) leads to

$$X_f=\left(\frac{c^2}{2\pi}\right)^2\left[-\left(\frac{1}{\pi}\arctan\frac{|c\xi_0|}{\beta\Gamma}\right)^2\frac{1}{\pi}\frac{\beta\Gamma}{\beta^2\Gamma^2+c^2\xi_0^2}+\frac{2}{\pi}\left(\arctan\frac{c|\xi_0|}{\beta\Gamma}\right)\frac{\beta\Gamma c|\xi_0|}{(\beta^2\Gamma^2+c^2\xi_0^2)^2}\right]. \tag{A9}$$

Here we have already dropped a third term, which is half the second term in the curly bracket in (A8). For $c\xi_0 \ll \beta\Gamma$, X_f is of the order of $c^4(c\xi_0)^2/(\beta\Gamma)^3$ and much smaller than X_f is of the order $c^2\beta\Gamma/\xi_0^2$ and much larger than the other diagrams.

*Work supported in part by the National Science Foundation.

†On leave from the Institut für Theoretische Physik, Köln, Germany with a research grant from the Deutsche Forschungsgemeinschaft.

[1]S. Q. Wang, W. E. Evenson, and J. R. Schrieffer, Phys. Rev. Letters 23, 92 (1969).

[2]W. E. Evenson, J. R. Schrieffer, and S. Q. Wang, J. Appl. Phys. 41, 1199 (1970).

[3]J. R. Schrieffer (unpublished).

[4]B. Mühlschlegel (unpublished).

[5]D. R. Hamann, Phys. Rev. Letters 23, 95 (1969).

[6]R. L. Stratonovich, Dokl. Akad. Nauk SSSR 115, 1097 (1957) [Soviet Phys. Doklady 2, 416 (1958)].

[7]J. Hubbard, Phys. Rev. Letters 3, 77 (1959).

[8]B. Mühlschlegel, J. Math. Phys. 3, 522 (1962).

[9]The most general treatment of a many-body system in this way has been described by J. Zittartz, Z. Physik 180, 219 (1964).

[10]Such an approach has been used by Hamann for the Anderson model in Ref. 5 and has recently been extended by him: D. R. Hamann, Phys. Rev. B 2, 1373 (1970).

[11]M. Gaudin, Nucl. Phys. 20, 513 (1960); J. S. Langer, Phys. Rev. 134, A553 (1964).

[12]J. R. Schrieffer and D. C. Mattis, Phys. Rev. 140, A1412 (1965).

[13]B. Kjöllerström, D. J. Scalapino, and J. R. Schrieffer, Phys. Rev. 148, 665 (1966).

[14]L. Dworin, Phys. Rev. 177, 426 (1969).

[15]For notations compare, e.g., A. A. Abrikosov, L. P. Gorkov, and L. I. Dzyaloshinskii, *Quantum Field Theory Methods in Statistical Physics* (Prentice-Hall, Englewood Cliffs, N. J., 1963).

[16]D. J. Scalapino, Phys. Rev. Letters 16, 937 (1966).

[17]The following considerations follow very closely the treatment for the interacting electron gas, given by V. Ambegaokar, *Astrophysics and the Many Body Problem* (Benjamin, New York, 1963).

[18]The corresponding formula (33) for the interacting electron gas has first been derived by J. M. Luttinger and J. C. Ward, Phys. Rev. 118, 1417 (1960); that this formula does not only give self-consistent, but also conserving, approximations has been shown by G. Baym, Phys. Rev. 127, 1391 (1962).

[19]For details see Refs. 1–3.

[20]J. M. Luttinger and J. C. Ward, Phys. Rev. 118, 1417 (1960).

[21]J. R. Schrieffer and S. Q. Wang (unpublished).

[22]B. Mühlschlegel and J. Zittartz, Z. Physik. 175, 553 (1963).

[23]J. R. Schrieffer and P. A. Wolff, Phys. Rev. 149, 491 (1966).

[24]L. Dworin, Phys. Rev. 164, 818 (1967); 164, 841 (1967).

[25]See, e.g., M. Abramowitz and I. A. Stegun, *Handbook of Mathematical Functions* (Dover, New York 1965), Chap. 6.

PHYSICAL REVIEW B VOLUME 2, NUMBER 9 1 NOVEMBER 1970

Spin-Wave Relaxation in EuS†

R. R. Bartkowski*
Gordon McKay Laboratories, Harvard University, Cambridge, Massachusetts 02138
(Received 25 May 1970)

As part of a study of spin-wave relaxation, spin-wave linewidths have been measured in EuS. EuS is a good candidate for this study because of its high saturation magnetization, $4\pi M = 14\,000$ G at $T = 0$ °K and small exchange energy which is reflected in its Curie temperature, $T_C = 16$ °K. The linewidths due to three-spin-wave dipole-dipole interactions are large ranging up to 100 Oe. The theory of three-spin-wave relaxation processes explains the linewidths observed both in relation to different spin waves at a fixed temperature and temperature dependence for a given spin wave over the range measured, i.e., 2–6 °K.

I. INTRODUCTION

Materials which have a high magnetization offer a new area for the study of spin-wave relaxation effects. Since the magnetic dipole-dipole interaction in these materials is strong, we expect that relaxation processes associated with this interaction will contribute significantly. EuS which has a saturation magnetization of 14 000 G at $T = 0$ °K is a good candidate for this study. In this compound,